Reassessing the role of stochastic forcing in the 1997–1998 El Niño

G. A. Vecchi,[1,2] A. T. Wittenberg,[1] and A. Rosati[1]

Received 26 September 2005; revised 28 November 2005; accepted 1 December 2005; published 14 January 2006.

[1] We explore the extent to which stochastic atmospheric variability was fundamental to development of extreme sea surface temperature anomalies (SSTAs) during the 1997–8 El Niño. The observed western equatorial Pacific westerly zonal stress anomalies (τ_a^x), which appeared between Nov. 1996 and May 1997 as a series of episodic bursts, were largely reproducible by an atmospheric general circulation model (AGCM) ensemble forced with observed SST. Retrospective forecasts using a hybrid coupled model (HCM) indicate that coupling only the part of τ_a^x linearly related to large-scale tropical Pacific SSTA is insufficient to capture the observed 1997 warming; but, accounting in the HCM for all the τ_a^x that was connected to SST, recovers most of the strong SSTA warming. The AGCM-estimated range of stochastic τ_a^x forcing induces substantial dispersion in the forecasts, but does not obscure the large-scale warming in most HCM ensemble members. **Citation:** Vecchi, G. A., A. T. Wittenberg, and A. Rosati (2006), Reassessing the role of stochastic forcing in the 1997–1998 El Niño, *Geophys. Res. Lett.*, *33*, L01706, doi:10.1029/2005GL024738.

1. Introduction

[2] The extent to which the El Niño-Southern Oscillation (ENSO) phenomenon is influenced by stochastic processes has implications for both its potential predictability and its response to background changes [e.g., *Barnett et al.*, 1993; *Penland and Sardeshmukh*, 1995; *Fedorov et al.*, 2003; *Philander and Fedorov*, 2003]. We focus on a particular stochastic process: internal atmospheric variability unconstrained by low-frequency SST. In particular, equatorial westerly wind events (WWEs) [*Luther et al.*, 1983; *Giese and Harrison*, 1991; *Harrison and Vecchi*, 1997] are associated with eastern equatorial Pacific (EEqP) waveguide warming [*Vecchi and Harrison*, 2000]; both directly (via equatorial Kelvin pulses) and through coupled air-sea feedbacks [e.g., *Giese and Harrison*, 1991; *Vecchi*, 2000; *Lengaigne et al.*, 2003, 2004a, 2004b]. The large amplitude of the 1997–8 El Niño has been connected with enhanced occurrence of WWEs prior to its onset [e.g., *McPhaden*, 1999; *Lengaigne et al.*, 2003].

[3] Individual WWEs are associated with a range of phenomena: the Madden-Julian Oscillation, tropical cyclones, mid-latitude cold surges, etc. While often viewed as stochastic forcing for ENSO, aspects of WWEs are not "noise-like": on average WWEs are preceded by large-scale SSTA patterns [*Vecchi and Harrison*, 2000], inter-WWE separation is not that of a memory-less process [*Vecchi*, 2000], WWEs can induce subsequent WWEs [*Lengaigne et al.*, 2003, 2004a, 2004b], and WWEs follow the location of warmest SST [*Yu et al.*, 2003; *Vecchi*, 2006]. It has been hypothesized that WWEs may be linked to SST [*Vecchi*, 2000; *Wittenberg*, 2002; *Lengaigne et al.*, 2003, 2004a; *Yu et al.*, 2003; *Vecchi*, 2006], and *Lengaigne et al.* [2003, 2004a] showed that some WWEs in a developed El Niño represent a high-frequency aspect of the low-frequency coupled evolution. *Eisenman et al.* [2006] coupled WWEs to warm pool extent, and find that this nonlinear air-sea feedback amplifies El Niño in an intermediate-complexity model. A focus of our paper is the WWE enhancement prior to the development of large-scale "El Niño" SSTA.

[4] We focus on the 1997–8 El Niño event because of: i) its large amplitude [*McPhaden*, 1999], ii) the failure of many forecast systems to capture its onset, growth and amplitude [*Barnston et al.*, 1999; *Landsea and Knaff*, 2000], and iii) the hypothesized role of stochastic atmospheric forcing in its development and unpredictability. We investigate the extent to which wind stresses for this event may have represented a forcing independent of SST, a linear response to large-scale tropical Pacific SSTA, or some other type of SST-forced response; and we examine the implications of these various components for retrospective forecasts of the event.

2. Models

2.1. Atmospheric General Circulation Model (AGCM)

[5] We use a version of the NOAA-GFDL global AGCM/land model, AM2/LM2. The model configuration and climate characteristics are described by the *GFDL Global Atmospheric Model Development Team* [2004]. A ten-member ensemble of 52-year runs (1951–2002) is forced by the global monthly 1° × 1° SST and sea ice data prepared by J. Hurrell (2003, provided by NCAR); different initial conditions are used for each ensemble member. Generally, the circulation over the tropical Pacific, its relationship to ENSO, and the ENSO mid-latitudes teleconnections are well represented by this model [*GFDL Global Atmospheric Model Development Team*, 2004; *Wittenberg et al.*, 2006; *Vecchi*, 2006]. The notation $\langle\Psi\rangle$ denotes the ensemble-mean of a variable Ψ, and Ψ^* denotes an ensemble member's departure from $\langle\Psi\rangle$.

2.2. Linear Statistical Atmospheric Model (LSAM)

[6] We wish to partition the stress anomaly vector, $\boldsymbol{\tau}_a$, into a component that is controlled by SST and one arising from internal atmospheric processes:

$$\boldsymbol{\tau}_a = \boldsymbol{F}(SST) + \boldsymbol{N} \tag{1}$$

[1]NOAA/Geophysical Fluid Dynamics Laboratory, Princeton, New Jersey, USA.

[2]Visiting scientist from University Corporation for Atmospheric Research, Boulder, Colorado, USA.

0094-8276/06/2005GL024738$05.00

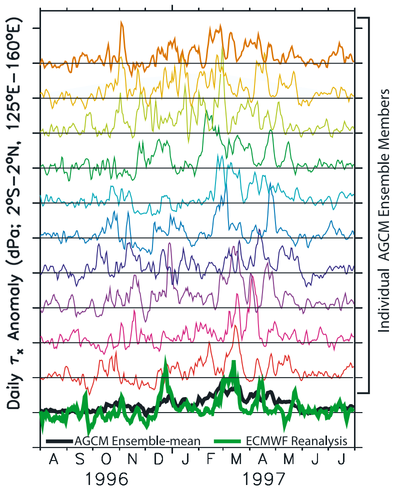

Figure 1. WEqP daily τ_a^x from ERA40, AGCM ensemble-mean, and each ensemble member. Horizontal lines mark zero value, distance between ticks on axis represents 1 dPa.

[7] Given an AGCM ensemble forced by observed SST, we may approximate this partitioning as $\boldsymbol{F}(SST) = \langle \boldsymbol{\tau_a} \rangle$ and $\boldsymbol{N} = \boldsymbol{\tau_a^*}$; an approximation that should improve with increasing ensemble size. Unfortunately, this procedure is impossible with observations, where only one realization is available; an often-used alternative is to decompose $\boldsymbol{\tau_a}$ using a linear statistical atmospheric model (LSAM) [e.g., *Zavala-Garay et al.*, 2003; *Batstone and Hendon*, 2005]. An LSAM approximates the relationship between SST and $\boldsymbol{\tau_a}$ by regressing $\boldsymbol{\tau_a}$ onto a set of SSTA predictors, so that (1) becomes:

$$\boldsymbol{\tau_a} = \boldsymbol{\mathcal{L}}(P(SSTA)) + \boldsymbol{E} = \boldsymbol{\mathcal{L}}(P(SSTA)) + \langle \boldsymbol{E} \rangle + \boldsymbol{\tau_a^*} \qquad (2)$$

where $\boldsymbol{\mathcal{L}}$ is a linear operator on the set of predictors, P, and $\boldsymbol{E}$ is a residual from $\boldsymbol{\tau_a}$ that is uncorrelated with P. For the observational record or a single AGCM ensemble member, $\boldsymbol{E}$ includes both the ensemble-mean residual ($\langle \boldsymbol{E} \rangle$), which represents the SST-forced variability of $\boldsymbol{\tau}_\mathrm{a}$ not captured by a linear regression onto large-scale tropical Pacific SSTA, and the true stochastic component ($\boldsymbol{\tau}_\mathrm{a}^*$). We build an LSAM on the AGCM ensemble-mean to compute $\mathcal{L}$ and $\langle \boldsymbol{E} \rangle$ (computing the ensemble-mean of LSAMs built from individual ensemble members gives very similar results). We focus on τ_a^x, so scalar notation denotes the zonal component of a vector; e.g., $E = \boldsymbol{E} \bullet \boldsymbol{\hat{\imath}}$.

[8] We use the LSAM described by *Zhang et al.* [2005], which is similar to that of *Harrison et al.* [2002] and *Wittenberg* [2002], and apply it to the 1979–2002 monthly AGCM $\boldsymbol{\tau_a}$. We build the LSAM over these dates in order to coincide with the satellite period. First, we compute P using singular value decomposition (SVD) of the tropical Pacific SSTA/$\boldsymbol{\tau_a}$ covariance matrix; here we use the 7 leading SST modes, though the results are qualitatively robust using a wide range of modes (3–21). $\mathcal{L}$ is computed by linearly regressing the $\boldsymbol{\tau_a}$ field onto P.

2.3. Hybrid Coupled Model (HCM)

[9] A hybrid coupled ocean-atmosphere model is built by coupling the LSAM to the GFDL Modular Ocean Model v.4 (MOM4) [*Griffies et al.*, 2005]. MOM4 is configured with 25 vertical levels (~15 m resolution above 150 m); the global horizontal resolution is uniform 2° zonal, and 0.5° meridional near-Equator, telescoping to 5° near the poles. Model configuration, initialization and coupling are as in the work by *Zhang et al.* [2005]. The HCM surface enthalpy and freshwater fluxes include prescribed climatological "flux adjustments" to maintain a realistic background state.

3. Results

3.1. Westerly Wind Events Preceding the 1997–8 El Niño

[10] The evolution of the late-1996/early-1997 western equatorial Pacific (WEqP, 2°S–2°N 130°E–160°E) τ_a^x is shown in Figure 1 – these latitudes highlight the oceanic equatorial waveguide. WEqP westerly τ_a^x is evident in both the ECMWF Reanalysis-40 (ERA40) and the AGCM ensemble-mean; and occurs just prior to the warming of the EEqP (Figure 2a). In ERA40 the westerlies arise as a series of equatorial WWEs between Nov. 1996 and May 1997; every ensemble-member exhibits seasonal-mean westerly τ_a^x. In each AGCM ensemble member and ERA40 the low-frequency westerly τ_a^x arises as a series of skewed WWEs. The ensemble-mean τ_a^x is relatively steady through the period.

[11] Each individual WWE at the onset of the El Niño was associated with internal atmospheric variability; yet, the enhancement of WWEs is reproducible given the observed SST. For observations, each of the AGCM ensemble members, and the AGCM ensemble-mean, the westerly anomalies in Nov. 1996–May 1997 were associated with an eastward extension of convection into the western and central Pacific (not shown); there was also an increase in convective variability, expressed in the episodic nature of the τ_a^x. *Zavala-Garay et al.* [2005] show that the sub-seasonal details of the τ_a^x variability do not impact the interannual evolution of the coupled system as much as the interannual anomalies do; so henceforth we focus on the interannual variability of τ_a^x (monthly τ_a^x smoothed by a 5-month triangle).

3.2. Statistical Decomposition of AGCM Ensemble

[12] We here assess the effectiveness of the LSAM decomposition of τ_a^x (see Section 2.2) within the AGCM framework. The AGCM does a reasonable job representing the ERA40 interannual variability of τ_a^x during 1996–1998, although the AGCM does overestimate the amplitude of the central equatorial Pacific (CEqP) τ_a^x variability (compare Figures 2b and 2d). Both ERA40 and the AGCM show westerly τ_a^x in the WeqP prior to EEqP SSTAs warming, and strong westerly τ_a^x extended across much of the CEqP at the height of the El Niño. The slow eastward propagation of westerly τ_a^x is captured by the AGCM.

[13] The linear model of the AGCM $\langle \tau_a^x \rangle$ (Figure 2d) captures most of the interannual τ_a^x variability near the Equator (over 80% of the interannual variance 1979–2001). However, a substantial part of the SST-forced τ_a^x variability over the WEqP is not captured by the LSAM, $\langle E \rangle$. From Nov. 1996–May 1997, $\langle E \rangle$ is westerly over the WEqP, and easterly $\langle E \rangle$ develops during the period of peak warm EEqP SSTA.

[14] It is interesting to compare the spatial structure of τ_a^{x*} from a single ensemble member to that of $\langle E \rangle$

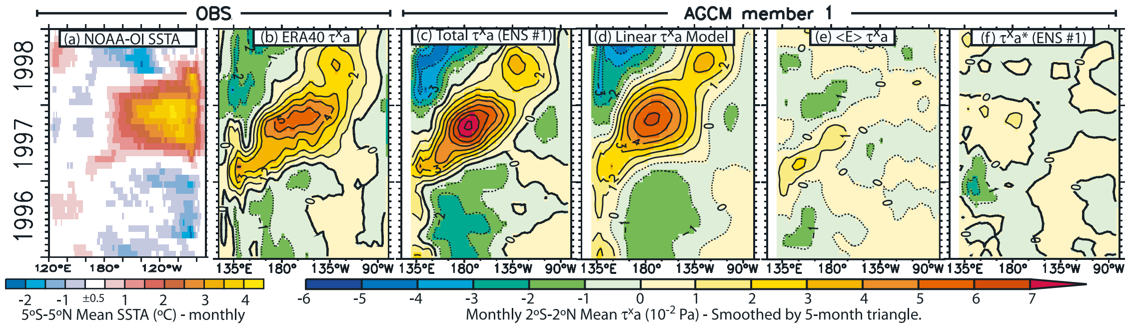

Figure 2. Monthly near-equatorial Pacific (a) *Reynolds et al.* [2002] SSTA (°C, from 1981–2002 climatology); and time-filtered, τ_a^x from (b) ERA40, AGCM: (c) total from ensemble member 1 (d) ensemble-mean $\mathcal{L}$, (e) $\langle E\rangle$, and (f) ensemble member 1 ${\tau_a}^{*x}$ (cPa, from respective 1951–2000 climatology).

(Figure 2e vs 2f). The largest amplitudes of both $\langle E\rangle$ and ${\tau_a}^{x*}$ are west of the Dateline; for any ensemble member, at a given place and time, the amplitude of ${\tau_a}^{x*}$ can be larger than that of $\langle E\rangle$, but the time- and space-scales ${\tau_a}^{x*}$ are shorter than those of $\langle E\rangle$. Over 1979–2002 the interannual variance of WEqP $\langle E\rangle$ is comparable to that of ${\tau_a}^{x*}$ from the various members, and since $\langle E\rangle$ and ${\tau_a}^{x*}$ are uncorrelated:

$$\sigma^2(E) = \sigma^2(\langle E\rangle) + \sigma^2({\tau_a}^{x*}) \tag{3}$$

[15] Applying the LSAM to any ensemble member recovers E, which for this particular AGCM overestimates the interannual near-equatorial ${\tau_a}^{x*}$ variance by a factor of 2.

3.3. Impact on Coupled Forecasts

[16] To explore impacts of the LSAM residuals on this El Niño, we use an experimental forecast system built around the HCM (see Section 2.3). Figure 3 shows results of one-year retrospective forecasts initialized in Jan. 1997. First, we performed a linear deterministic forecast (FCST-A, dotted line), in which no external forcing is applied to the HCM. In FCST-A, EEqP SSTA shows a gradual warming through boreal spring and summer, indicating that the initial conditions contained some preconditioning for warming. Yet this linear forecast greatly underestimates the actual warming (solid line): something important is missing from the forecast system.

[17] Two additional forecast experiments are used to isolate the effects of forcing by the τ_a^x residuals from the LSAM. (Since there is SST-information in the applied forcing, neither of experiment FCST-B or FCST-C represents an operational forecast framework.) We performed a forecast (FCST-B, blue squares) applying $\langle E\rangle$ as an external forcing on the HCM: $\langle E\rangle$ had a substantial impact on the HCM's ability to produce the El Niño warming. By the El Niño peak, Dec. 1997, FCST-B recovers about 70% of the observed NIÑO3.4; NIÑO3.4 is 1°C warmer in FCST-B than in FCST-A. The difference between FCST-A and FCST-B is due both to the direct forcing from the westerly $\langle E\rangle$, and to coupled feedbacks arising from the $\langle E\rangle$-driven SSTA. We note that $\langle E\rangle$ is not equivalent to a linear coupling coefficient applied to $\boldsymbol{\mathcal{L}}$: the relationship of $\langle E\rangle$ and $\mathcal{L}$ to SST is different, and $\langle E\rangle$ is orthogonal to $\mathcal{L}$.

[18] To investigate the impact of ${\tau_a}^{x*}$ we run an ensemble of ten additional forecasts, in which both $\langle E\rangle$ and the ten realizations of ${\tau_a}^{x*}$ act as external forcing on the HCM (FCST-C, red symbols). Stochastic atmospheric variability induces substantial dispersion in the forecast ensemble: of the ensemble members, one shows a very weak warming and one exceeds the observed warming. The gap between the two coldest forecasts and the rest raises the possibility that the size of the ensemble (10) may not span the full range of stochastic variability; as resources become available, larger ensembles should be run. Despite the dispersion, 9 of 10 ensemble members show warming larger than that of FCST-A (6 of 10 at least 1°C warmer): much of the impact of $\langle E\rangle$ is not obscured by stochastic forcing. The HCM response to stochastic forcing is fairly linear, in that both the mean and the median of the ensemble of FCST-C track FCST-B.

4. Discussion

[19] Using a hierarchy of modeling experiments, we have explored the role of stochastic atmospheric forcing in the development of the 1997–8 El Niño. Both the mean westerly τ_a^x and enhancement of WWE activity between Nov. 1996 and May 1997 was the deterministic response of an AGCM ensemble to the observed SST field (Section 3.1). The error in a LSAM estimate of interannual WEqP stochastic τ_a^x

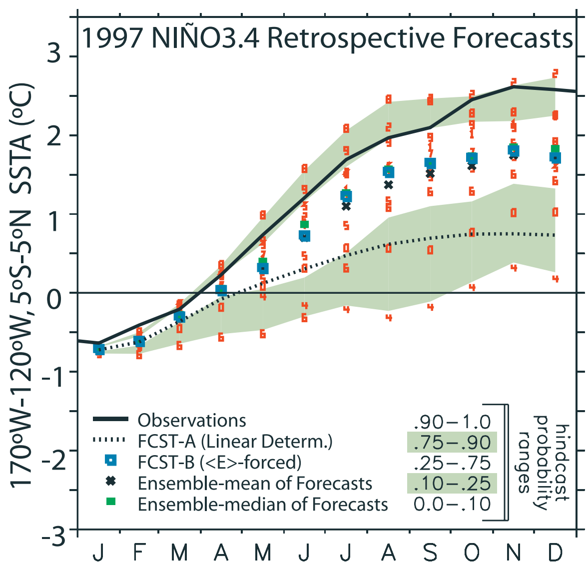

Figure 3. Retrospective forecasts of NIÑO3.4 SSTA, see Section 3.3. Red symbols show FCST-C.

variability is as large as the stochastic variability itself (Section 3.2). A series of retrospective forecasts indicate that the part of τ_a^x linearly related to large-scale SSTA was not sufficient to explain the warming in 1997; but when we include all parts of τ_a^x that could be related to SST, most of the EEqP warming in 1997 is recovered (Section 3.3). The observed warming is not obscured by the ensemble estimate of stochastic τ_a^x forcing (Figure 3).

[20] LSAM estimates have been used to explore issues of predictability of the ENSO system [e.g., *Barnett et al.*, 1993; *Eckert and Latif*, 1997; *Moore and Kleeman*, 1999; *Harrison et al.*, 2002; *Zavala-Garay et al.*, 2003, 2005] and ENSO's sensitivity to parameter changes [*Syu et al.*, 1995; *Wittenberg*, 2002]. In our AGCM framework, the LSAM recovers most of the SST-forced τ_a^x signal, however the error ($\langle E \rangle$) is influential in our forecasts. LSAM overestimates the variance of τ_a^{x*}, and the LSAM. The LSAM partitioning may be problematic for assessing the role of stochastic processes in ENSO; nonlinear statistical [*Li et al.*, 2005] or dynamical approaches may yield a better partitioning of the coupled and stochastic components of stress.

[21] The 1997–8 El Niño was of quite unusual amplitude and evolution; since all El Niños are unique to some degree, the general applicability of our findings must be explored further. The roles of noise and nonlinearity in other ENSO events, and of particular SSTA patterns in the enhancement of WWE activity in the WEqP, will be addressed later in a more in-depth article.

[22] We have shown that much of the strong westerly τ_a^x and WWE enhancement at the onset of the 1997–8 El Niño cannot be considered "atmosphere-only noise", as it is reproducible in an AGCM ensemble forced by SST. However, this does not rule out the possible impact of stochastic variability of the *coupled* system. In the same way the impact of $\langle E \rangle$ was enhanced by coupling (Section 3.3), coupling could enhance stochastic atmospheric forcing; or some fraction $\langle E \rangle$ could have arisen due to unpredictable details in the state of the coupled system, representing a stochastic coupled mode of variability.

[23] The rapidity and amplitude of the warming in the 1997–8 El Niño event was underestimated by most forecast systems operational at the time, and stochastic atmospheric variability has been suggested as a possible reason for this forecast difficulty. But our analysis indicates that an important part of the τ_a^x variability often interpreted as stochastic was actually linked to SST – was it perhaps predictable? Further studies should explore this exciting possibility.

[24] **Acknowledgments.** GAV is supported by the UCAR/VSP at NOAA/GFDL. We are grateful to R. Gudgel, I. Held, N.-C. Lau, S. Ilcane, J. Zavala-Garay and two anonymous reviewers.

References

Barnett, T. P., et al. (1993), ENSO and ENSO-related predictability. part I: Prediction of equatorial Pacific sea surface temperature with a hybrid coupled ocean–atmosphere model, *J. Clim.*, *6*, 1545–1566.
Barnston, A. G., M. H. Glantz, and Y. He (1999), Predictive skill of statistical and dynamical climate models in SST forecast during the 1997–98 El Niño episode and the 1998 La Niña onset, *Bull. Am. Meteorol. Soc.*, *80*, 217–243.
Batstone, C., and H. H. Hendon (2005), Characteristics of stochastic variability associated with ENSO and the role of the MJO, *J. Clim.*, *18*, 1773–1789.
Eckert, C., and M. Latif (1997), Predictability of a stochastically forced hybrid coupled model of El Niño, *J. Clim.*, *10*, 1488–1504.
Eisenman, I., L. Yu, and E. Tziperman (2006), Westerly wind bursts: ENSO's tail rather than the dog?, *J. Clim.*, in press.
Fedorov, A. V., S. L. Harper, S. G. Philander, B. Winter, and A. Wittenberg (2003), How predictable is El Nino?, *Bull. Am. Meteorol. Soc.*, *84*, 911–919.
GFDL Global Atmospheric Model Development Team (2004), The new GFDL global atmosphere and land model AM2-LM2: Evaluation with prescribed SST simulations, *J. Clim.*, *17*, 4641–4673.
Giese, B. S., and D. E. Harrison (1991), Eastern equatorial Pacific response to three composite westerly wind types, *J. Geophys. Res.*, *96*, 3239–3248.
Griffies, S. M., et al. (2005), Formulation of an ocean model for global climate simulations, *Ocean Sci.*, *1*, 45–79.
Harrison, D. E., and G. A. Vecchi (1997), Westerly wind events in the tropical Pacific: 1986–1995, *J. Clim.*, *10*, 3131–3156.
Harrison, M. J., A. Rosati, B. J. Soden, E. Galanti, and E. Tziperman (2002), An evaluation of air-sea flux products for ENSO simulation and prediction, *Mon. Weather Rev.*, *130*, 723–732.
Landsea, C. W., and J. A. Knaff (2000), How much skill was there in forecasting the very strong 1997–98 El Niño?, *Bull. Am. Meteorol. Soc.*, *81*, 2107–2119.
Lengaigne, M., et al. (2003), The March 1997 westerly wind event and the onset of the 1997/98 El Niño: Understanding the role of the atmospheric response, *J. Clim.*, *16*, 3330–3343.
Lengaigne, M., et al. (2004a), Triggering of El Niño by westerly wind events in a coupled general circulation model, *Clim. Dyn.*, *23*, 601–620.
Lengaigne, M., J.-P. Boulanger, C. Menkes, P. Delecluse, and J. Slingo (2004b), Westerly wind events in the tropical Pacific and their influence on the coupled ocean-atmosphere system: A review, in *Earth Climate: The Ocean-Atmosphere Interaction*, *Geophys. Monogr. Ser.*, vol. 147, pp. 49–69, AGU, Washington, D. C.
Li, S. Y., W. W. Hsieh, and A. M. Wu (2005), Hybrid coupled modeling of the tropical Pacific using neural networks, *J. Geophys. Res.*, *110*, C09024, doi:10.1029/2004JC002595.
Luther, D. S., D. E. Harrison, and R. A. Knox (1983), Zonal winds in the central equatorial Pacific and El Nino, *Science*, *222*, 327–330.
McPhaden, M. J. (1999), Genesis and evolution of the 1997–98 El Niño, *Science*, *283*, 950–954.
Moore, A. M., and R. Kleeman (1999), Stochastic forcing of ENSO by the intraseasonal oscillation, *J. Clim.*, *12*, 1199–1220.
Penland, C., and P. D. Sardeshmukh (1995), The optimal growth of tropical sea surface temperature anomalies, *J. Clim.*, *8*, 1999–2024.
Philander, S. G., and A. Fedorov (2003), Is El Niño sporadic or cyclic?, *Annu. Rev. Earth Planet. Sci.*, *31*, 579–594.
Reynolds, R. W., N. A. Rayner, T. M. Smith, D. C. Stokes, and W. Wang (2002), An improved in situ and satellite SST analysis for climate, *J. Clim.*, *15*, 1609–1625.
Syu, H.-H., J. D. Neelin, and D. Gutzler (1995), Seasonal and interannual variability in a hybrid coupled GCM, *J. Clim.*, *8*, 2121–2143.
Vecchi, G. A. (2000), Tropical Pacific sub-seasonal wind variability and El Niño, Ph.D. dissertation, 187 pp., Univ. of Wash., Seattle.
Vecchi, G. A. (2006), The termination of the 1997–98 El Niño part II: Mechanisms of atmospheric change, *J. Clim.*, in press.
Vecchi, G. A., and D. E. Harrison (2000), Tropical Pacific sea surface temperature anomalies, El Niño and equatorial westerly wind events, *J. Clim.*, *13*, 1814–1830.
Wittenberg, A. T. (2002), ENSO response to altered climates, Ph.D. thesis, 475 pp., Princeton Univ., Princeton, N. J.
Wittenberg, A. T., et al. (2006), GFDL's CM2 global coupled climate models—part 3: Tropical Pacific climate and ENSO, *J. Clim.*, in press.
Yu, L., R. A. Weller, and W. T. Liu (2003), Case analysis of a role of ENSO in regulating the generation of westerly wind bursts in the Western Equatorial Pacific, *J. Geophys. Res.*, *108*(C4), 3128, doi:10.1029/2002JC001498.
Zavala-Garay, J., A. M. Moore, C. L. Perez, and R. Kleeman (2003), The response of a coupled model of ENSO to observed estimates of stochastic forcing, *J. Clim.*, *16*, 2827–2842.
Zavala-Garay, J., C. Zhang, A. M. Moore, and R. Kleeman (2005), The linear response of ENSO to the Madden–Julian Oscillation, *J. Clim.*, *18*, 2441–2459.
Zhang, S., et al. (2005), Tropical Pacific ocean data assimilation using a parallelized ensemble filter with a stochastic hybrid coupled GCM, *Mon. Weather Rev.*, *133*, 3176–3201.

A. Rosati, G. A. Vecchi, and A. T. Wittenberg, NOAA/GFDL, Princeton Forrestal Campus Rte. 1, P.O. Box 308, Princeton, NJ 08542-0308, USA. (gabriel.a.vecchi@noaa.gov)